ISBN: 978-3-95450-184-7 doi:10.18429/JACoW-IPAC2018-THPMF082

SUPPRESSION OF MICROBUNCHING INSTABILITY USING A QUADRUPOLE INSERTED CHICANE IN FREE-ELECTRON-LASER LINACS

Biaobin Li[1], Ji Qiang*, Lawrence Berkeley National Laboratory, 94720 Berkeley, USA
[1]also at University of Science and Technology of China, 230029 Hefei, China

Abstract

The microbunching instability (MBI) driven by beam collective effects in a linear accelerator of a free-electron laser (FEL) facility can significantly degrade the electron beam quality and FEL performance. A method exploited longitudinal mixing derived from the natural transverse spread of the beam was proposed several years ago using two dipoles to suppress the instability. In this paper, instead of using bending magnets to introduce the transverse-to-longitudinal coupling, which will lead to an inconvenient deflection of the downstream beam line, we propose a scheme using a quadrupole inserted chicane to introduce the longitudinal mixing inside the accelerator transport system to suppress this instability. And we finally eliminate the transverse-to-longitudinal coupling after the dogleg section.

INTRODUCTION

The microbunching instability in linacs can limit the performance of single-pass x-ray FELs by significantly degrading the beam quality [1–5]. The conventional method to control the instability is using a laser heater to enlarge the beam uncorrelated energy spread [2,6], which is typically tolerable for operation of self-amplified spontaneous emission (SASE) FELs, but for seeded FELs it could limit the FEL gain to some degree [7]. The later proposed reversible heating device based on two transverse deflecting rf structures (TDSs) can suppress the microbunching instability without sacrificing the beam brightness as the introduced energy spread is eliminated in the second TDS [8]. However, this scheme would be quite expensive and complicated. Instead of exploiting longitudinal mixing from large beam energy spread, but from the natural transverse spread of the beam, schemes based on bending magnets is proposed [9]. And then schemes introducing both energy spread and transverse-to-longitudinal phase space coupling based on transverse gradient undulator (TGU) are proposed [10–12]. The scheme based on bending magnets is simple and can preserve the longitudinal beam brightness without expensive hardware. However the using of bending magnets will change the beam line direction which is not convenient and difficult to apply to the existing FEL facilities.

In this paper, we propose a scheme which would keep the advantages of using bending magnets but avoid the inconvenient deflection of the downstream beam line by inserting quadrupoles in a four dipoles chicane to introduce the longitudinal mixing to suppress the instability. And we finally eliminate the transverse-to-longitudinal coupling after the dogleg section, which makes our whole transportation line achromatic. In the following sections, we will give a potential accelerator model to illustrate this method. The lattice design is based on First-order transfer matrix in $(x, x', y, y', z, \delta)$ phase space and performed with the help of Elegant [13]. And then microbunching gain calculation based on staged amplification theory [14] is given to show the suppression effects.

OVERVIEW OF THE SCHEME

Figure 1 shows a potential accelerator layout of the proposed scheme. We insert three quadrupoles in BC0 to introduce the transverse-longitudinal coupling terms R_{51} and R_{52} to suppress the MBI and to confine the transverse beam size. The quadrupole parameters are chosen to introduce larger longitudinal mixing terms and to maintain a small beam size, which is performed by particle swarm optimization [15], and the values of the coupling terms at the exit of BC0 $R_{51} = -1.37$, $R_{52} = -3.14$ m, $R_{56} = -0.105$ m are used for illustration. The electron beam is accelerated from the initial 100 MeV to 250 MeV at the exit of Linac-0, and then passes through BC1 providing 6 times compression. Linac-1 accelerates the beam to 1.5 GeV and then goes through BC2 providing a total compression factor as $C = 72$. The final beam energy is accelerated to 5 GeV in Linac-2 and the energy chirp is ramped down to zero at the entrance to the dogleg. The dogleg section, which consists of two dipole pair sandwiching three independent quadrupols [16], is designed to be isochronous and restore achromaticity at the same time, i.e. $R_{56}(s_{6\to7}) = 0$, $R_{16}(s_{0\to7}) = 0$, $R_{26}(s_{0\to7}) = 0$, which is performed with the help of Elegant by adjusting the qudrupole strengths [13].

The beam radius and energy evolutions are illustrated in Fig. 2. The initial electron beam transverse distribution is a uniform round cross section with 0.2 mm rms size and 0.4 mm mrad normalized transverse emittance with a flattop current of 15 A. The initial uncorrelated energy spread is 4 keV with zero energy chirp. Matching and FODO structures are used in the accelerator transport sections to control the beam transverse size. The maximum horizontal beam sizes in Linac-0, Linac-1, Linac-2 sections are about 1.3 mm, 0.9 mm, 0.5 mm respectively. Because of the dispersion leaked out from BC0 in the accelerator transport system, the horizontal direction beam size is much bigger than the vertical, which is still tolerable for the superconducting linac transport system. In the downstream of dogleg section, which consists of undulator section also based on

* jqiang@lbl.gov

ISBN: 978-3-95450-184-7 doi:10.18429/JACoW-IPAC2018-THPMF082

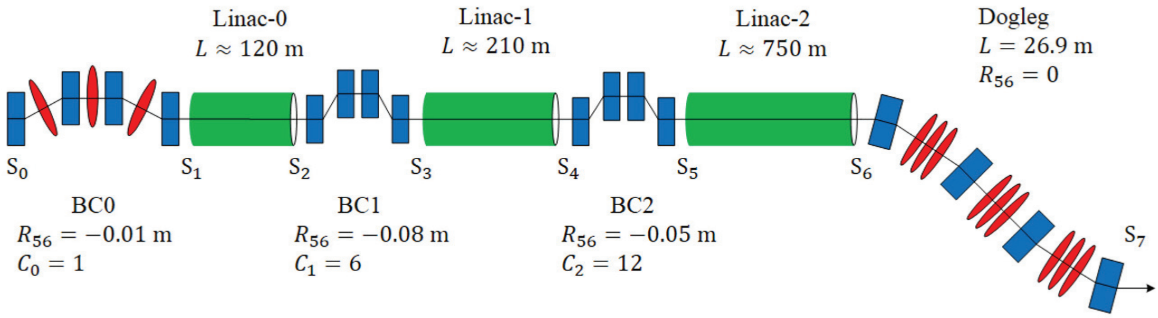

Figure 1: (color online). Scheme Layout. Quadrupoles are inserted in the middle position between dipoles. The momentum compaction factor of BC0 $R_{56} = -0.01$ m is in the case of the three quadrupoles turned off.

FODO structures, both horizontal and vertical beam sizes are periodic due to zero dispersion which is eliminated by the dogleg section.

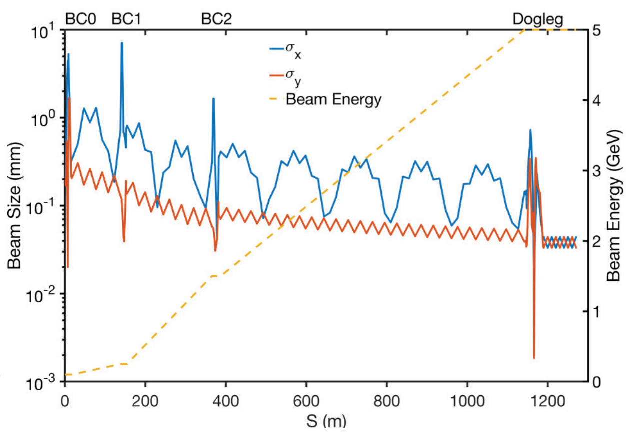

Figure 2: (color online). Evolution of the beam rms radius and energy along the longitudinal position.

MICROBUNCHING GAIN SUPPRESSION

Assuming an electron beam with an initial current modulation factor b_0 at the entrance (s_0) to BC0, the final modulation factor at the exit (s_7) of the dogleg section can be obtained by solving the microbunching integral equation provided in [4, 9], which takes acceleration effects into account. Neglecting collective effects inside all bending magnets and assuming electron beam is "frozen" in the linac sections, which means that electron longitudinal positions will not change when it is transferring through the linacs. The solution is given as

$$b[k(s_7); s_7] = b_1[k(s_7); s_7] + b_2[k(s_7); s_7] + b_3[k(s_7); s_7] + b_4[k(s_7); s_7] + b_5[k(s_7); s_7] + b_6[k(s_7); s_7], \tag{1}$$

where $k(s) = C(s)k_0$ and $C(s)$ is the compression factor $C(s) = 1/R_{55}(s)$, and k_0 is the initial modulation wave number. Here b_1 describes the evolution of the modulation factor in the absence of all collective effects, and is given as

$$b_1[k(s_7); s_7] = b_0 \exp[-k^2(s_7)\hat{R}_{56}^2(s_7)\sigma_{\delta_0}^2/2]; \tag{2}$$

the second term b_2 describes the amplification that the electron beam firstly get energy modulation due to the collective effects between s_1 and s_2 inside the accelerator system and then goes through the following section which provides the non-zero R_{56}, and is given as

$$b_2[k(s_7); s_7] = ib_0 k(s_7)\hat{R}_{56}(s_{1\to7})\frac{I(s_1)}{\gamma_0 I_A} \times \exp\left(\frac{-k_0^2\mathcal{D}^2(s_7)\sigma_{\delta_0}^2}{2}\right) \times \exp\left(\frac{-k_0^2\mathcal{H}\epsilon_{x,n}}{\gamma_0}\right)\int_{s_1}^{s_2}\frac{4\pi Z[k(\tau);\tau]}{Z_0}d\tau; \tag{3}$$

the third term b_3 describes the amplification that energy modulation comes from collective effects between s_3 and s_4, and is given as

$$b_3[k(s_7); s_7] = ib_0 k(s_7)\hat{R}_{56}(s_{3\to7})\frac{I(s_3)}{\gamma_0 I_A} \times \exp\left(\frac{-k_0^2\mathcal{D}^2(s_{3\to7})\sigma_{\delta_0}^2}{2}\right) \times \exp\left(\frac{-k_0^2\mathcal{H}\epsilon_{x,n}}{\gamma_0}\right)\int_{s_3}^{s_4}\frac{4\pi Z[k(\tau);\tau]}{Z_0}d\tau; \tag{4}$$

the fourth term b_4 describes the collective effects between s_5 and s_6 and is given as

$$b_4[k(s_7); s_7] = ib_0 k(s_7)\hat{R}_{56}(s_{5\to7})\frac{I(s_5)}{\gamma_0 I_A} \times \exp\left(\frac{-k_0^2\mathcal{D}^2(s_{5\to7})\sigma_{\delta_0}^2}{2}\right) \times \exp\left(\frac{-k_0^2\mathcal{H}\epsilon_{x,n}}{\gamma_0}\right)\int_{s_5}^{s_6}\frac{4\pi Z[k(\tau);\tau]}{Z_0}d\tau; \tag{5}$$

ISBN: 978-3-95450-184-7 doi:10.18429/JACoW-IPAC2018-THPMF082

the last two coupling terms describe the two and three stages amplification respectively, and are given as

$$\begin{aligned} b_5[k(s_7);s_7] = &-b_0 k(s_3)k(s_7)\hat{R}_{56}(s_{1\to3})\hat{R}_{56}(s_{3\to7}) \\ &\times \frac{I(s_1)I(s_3)}{(\gamma_0 I_A)^2}\exp\left(\frac{-k_0^2\mathcal{D}^2(s_{0\to3\to7})\sigma_{\delta_0}^2}{2}\right) \\ &\times \exp\left(\frac{-k_0^2\mathcal{H}\epsilon_{x,n}}{\gamma_0}\right)\int_{s_1}^{s_2}\frac{4\pi Z[k(\tau);\tau]}{Z_0}d\tau \\ &\times \int_{s_3}^{s_4}\frac{4\pi Z[k(\tau);\tau]}{Z_0}d\tau; \end{aligned} \tag{6}$$

$$\begin{aligned} b_6[k(s_7);s_7] = &-ib_0 k(s_3)k(s_5)k(s_7)\hat{R}_{56}(s_{1\to3}) \\ &\times \hat{R}_{56}(s_{3\to5})\hat{R}_{56}(s_{5\to7})\frac{I(s_1)I(s_3)I(s_5)}{(\gamma_0 I_A)^3} \\ &\times \exp\left(\frac{-k_0^2\mathcal{D}^2(s_{0\to3\to5\to7})\sigma_{\delta_0}^2}{2}\right) \\ &\times \exp\left(\frac{-k_0^2\mathcal{H}\epsilon_{x,n}}{\gamma_0}\right)\int_{s_1}^{s_2}\frac{4\pi Z[k(\tau);\tau]}{Z_0}d\tau \\ &\times \int_{s_3}^{s_4}\frac{4\pi Z[k(\tau);\tau]}{Z_0}d\tau \\ &\times \int_{s_5}^{s_6}\frac{4\pi Z[k(\tau);\tau]}{Z_0}d\tau. \end{aligned} \tag{7}$$

The damping to the modulation amplification terms $(b_2, b_3, b_4, b_5, b_6)$ is controlled by the exponents

$$\begin{aligned} \mathcal{D}^2(s_7) =& U^2(s_7,s_1) + C^2(s_1)\hat{R}_{56}^2(s_1), \\ \mathcal{D}^2(s_{3\to7}) =& U^2(s_7,s_3) + C^2(s_3)\hat{R}_{56}^2(s_3), \\ \mathcal{D}^2(s_{5\to7}) =& U^2(s_7,s_5) + C^2(s_5)\hat{R}_{56}^2(s_5), \\ \mathcal{D}^2(s_{0\to3\to7}) =& U^2(s_7,s_3) + U^2(s_3,s_1) + C^2(s_1)\hat{R}_{56}^2(s_1), \\ \mathcal{D}^2(s_{0\to3\to5\to7}) =& U^2(s_7,s_5) + U^2(s_5,s_3) + U^2(s_3,s_1) \\ &+ C^2(s_1)\hat{R}_{56}^2(s_1), \\ \mathcal{H} =& \frac{[\beta_{x0}\hat{R}_{51}(s_1) - \alpha_{x0}\hat{R}_{52}(s_1)]^2 + (\hat{R}_{52}(s_1))^2}{\beta_{x0}}, \end{aligned} \tag{8}$$

where $U(s,\tau) = C(s)\hat{R}_{56}(s) - C(\tau)\hat{R}_{56}(\tau)$, $I(s) = C(s)I_0$ and I_0 is the initial current, I_A is the Alfvén current, γ_0 is the initial relativistic factor, $\epsilon_{x,n}$ is the normalized horizontal emittance, β_{x0} and α_{x0} are the initial horizontal twiss parameters, σ_{δ_0} is the initial rms relative energy spread, $Z[k(\tau);\tau]$ is the impedance per unit length of collective effects and Z_0 is the vacuum impedance, $\hat{R}_{56}(\tau \to s) = R_{56}(\tau \to s)E_0/E(\tau)$, $\hat{R}_{51}(s_1) = R_{51}(s_1)$, $\hat{R}_{52}(s_1) = R_{52}(s_1)$ are converted from X phase space to $\hat{X}$ phase space in order to consider the acceleration effects following the definition [4]

$$\begin{aligned} x &= \hat{x}\sqrt{E_0/E(\tau)}, & x' &= \hat{x}'\sqrt{E_0/E(\tau)}, \\ y &= \hat{y}\sqrt{E_0/E(\tau)}, & y' &= \hat{y}'\sqrt{E_0/E(\tau)}, \\ z &= \hat{z}, & \delta &= \hat{\delta}E_0/E(\tau), \end{aligned} \tag{9}$$

where E_0 is the initial beam energy, and we used the shorthand notation $\hat{R}_{ij}(s) = \hat{R}_{ij}^{s_0\to s}$, where s_0 is the initial position. Obviously, the microbunching factor is damped not only from the initial energy spread and the function $\mathcal{D}$ but also from the longitudinal mixing associated with the initial horizontal emittance and the function $\mathcal{H}$ [4].

In order to avoid the three stages amplification of the microbunching, the dogleg section is designed to be isochronous, which will make microbunching factor b_4 and b_6 be zero. Following the parameters discussed in last section, Fig. 3 illustrates the final microbunching gain $|b[k(s_7);s_7]/b_0|$ driven by the longitudinal space charge impedance in the linac sections (see Eq. (21) in [17]). The microbunching gain is completely suppressed in the presence of BC0 section relative to the gain that is obtained when BC0 section is turned off.

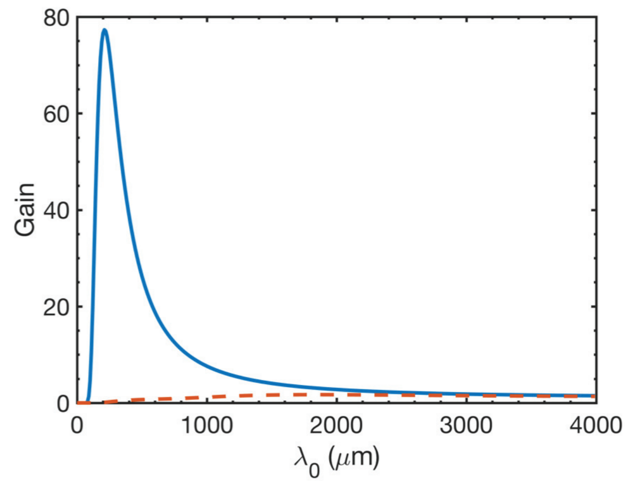

Figure 3: (color online). Microbunching gain spectrum at the final position (s_7) with (dashed line) and without (solid line) the use of the BC0 section. $\lambda_0 = 2\pi/k_0$ is the initial uncompressed modulation wavelength.

CONCLUSION

In this paper, microbunching instability suppression based on qudrupole magnets inserted in a chicane is proposed. The detailed accelerator design and theoretical analysis show that the scheme is feasible to suppress the instability completely. More detailed study including simulations using IMPACT [18] will be carried out in future work.

ACKNOWLEDGMENTS

This work was supported by the U.S. Department of Energy under Contract No. DE-AC02-05CH11231. One of the authors, B. L., thanks China Scholarship Council (CSC File No. 201706340072), the United States National Science Foundation, the Division of Physics of Beams of the American Physical Society, and TRIUMF for financial support, and also thanks Kilean Hwang for useful discussions.

ISBN: 978-3-95450-184-7 doi:10.18429/JACoW-IPAC2018-THPMF082

REFERENCES

[1] M Borland, YC Chae, P Emma, JW Lewellen, V Bharadwaj, WM Fawley, P Krejcik, C Limborg, SV Milton, and H-D Nuhn. Start-to-end simulation of self-amplified spontaneous emission free electron lasers from the gun through the undulator. *Nuclear Instruments and Methods in Physics Research Section A: Accelerators, Spectrometers, Detectors and Associated Equipment*, 483(1-2):268–272, 2002.

[2] EL Saldin, EA Schneidmiller, and MV Yurkov. Longitudinal space charge-driven microbunching instability in the tesla test facility linac. *Nuclear Instruments and Methods in Physics Research. Section A, Accelerators, Spectrometers, Detectors and Associated Equipment*, 528(1-2):355–359, 2004.

[3] Zhirong Huang, M Borland, P Emma, J Wu, C Limborg, G Stupakov, and J Welch. Suppression of microbunching instability in the linac coherent light source. *Physical Review Special Topics-Accelerators and Beams*, 7(7):074401, 2004.

[4] Marco Venturini. Microbunching instability in single-pass systems using a direct two-dimensional vlasov solver. *Physical Review Special Topics-Accelerators and Beams*, 10(10):104401, 2007.

[5] RA Bosch, KJ Kleman, and J Wu. Modeling two-stage bunch compression with wakefields: Macroscopic properties and microbunching instability. *Physical Review Special Topics-Accelerators and Beams*, 11(9):090702, 2008.

[6] Zhirong Huang, A Brachmann, F-J Decker, Y Ding, D Dowell, P Emma, J Frisch, S Gilevich, G Hays, and Ph Hering. Measurements of the linac coherent light source laser heater and its impact on the x-ray free-electron laser performance. *Physical Review Special Topics-Accelerators and Beams*, 13(2):020703, 2010.

[7] Li Hua Yu. Generation of intense uv radiation by subharmonically seeded single-pass free-electron lasers. *Physical Review A*, 44(8):5178, 1991.

[8] Christopher Behrens, Zhirong Huang, and Dao Xiang. Reversible electron beam heating for suppression of microbunching instabilities at free-electron lasers. *Physical Review Special Topics-Accelerators and Beams*, 15(2):022802, 2012.

[9] Ji Qiang, Chad E Mitchell, and Marco Venturini. Suppression of microbunching instability using bending magnets in free-electron-laser linacs. *Physical review letters*, 111(5):054801, 2013.

[10] Chao Feng, Dazhang Huang, Haixiao Deng, Qiang Gu, and Zhentang Zhao. Suppression of microbunching instability via a transverse gradient undulator. *New Journal of Physics*, 17(7):073028, 2015.

[11] Dazhang Huang, Chao Feng, Haixiao Deng, Qiang Gu, and Zhentang Zhao. Transverse to longitudinal phase space coupling in an electron beam for suppression of microbunching instability. *Physical Review Accelerators and Beams*, 19(10):100701, 2016.

[12] Tao Liu, Weilun Qin, Dong Wang, and Zhirong Huang. Reversible beam heater for suppression of microbunching instability by transverse gradient undulators. *Physical Review Accelerators and Beams*, 20(8):082801, 2017.

[13] Michael Borland. Elegant: A flexible sdds-compliant code for accelerator simulation. Report, Argonne National Lab., IL (US), 2000.

[14] Zhirong Huang and Kwang-Je Kim. Formulas for coherent synchrotron radiation microbunching in a bunch compressor chicane. *Physical Review Special Topics-Accelerators and Beams*, 5(7):074401, 2002.

[15] James Kennedy. *Particle swarm optimization*, pages 760–766. Springer, 2011.

[16] J Arthur, W Graves, M Renner, J Rosenzweig, G Faigel, Z Huang, M Wulff, J Hajdu, I Evans, K Kulander, et al. Linac coherent light source (lcls) conceptual design report. Technical report, 2002.

[17] J Qiang, RD Ryne, M Venturini, AA Zholents, and IV Pogorelov. High resolution simulation of beam dynamics in electron linacs for x-ray free electron lasers. *Physical Review Special Topics-Accelerators and Beams*, 12(10):100702, 2009.

[18] Ji Qiang, Robert D Ryne, Salman Habib, and Viktor Decyk. An object-oriented parallel particle-in-cell code for beam dynamics simulation in linear accelerators. *Journal of Computational Physics*, 163(2):434–451, 2000.